Journal of Academic Biology and Biology Education
Vol. 2, No. 1, June 2025, pp. 69~78
ISSN: 3062-9705, DOI: 10.37251/jouabe.v2i1.2016

Dual Gene Regulation by Hypoxia-Conditioned MSC Exosomes in a UV-B–Induced Collagen Loss Model: Targeting p21 and Cyclin D for Skin Regeneration

Riaflor Alcabedos[1], Ooi Siew Fong[2]
[1]Genetics and Molecular Biology Division, University of the Philippines Los Baños, Laguna, Philippines
[2]Department of Biological Science, Universiti Tunku Abdul Rahman, Kajang, Malaysia

Article Info

Article history:

Received Mar 30, 2025
Revised Apr 29, 2025
Accepted Jun 13, 2025
Online First Jun 22, 2025

Keywords:

Cyclin D
Exosomes
Mesenchymal Stem Cells (MSCs)
p21
UV-B–induced Collagen Loss

ABSTRACT

Purpose of the study: This study aims to investigate the effect of hypoxia-conditioned MSC-derived exosomes (E-MSCs) on the expression of p21 and Cyclin D genes in a UV-B-induced collagen loss mouse model, using in vivo experiments and gene expression analysis.

Methodology: This in vivo experimental study used a Post-Test Only Control Group Design with male Wistar rats (Rattus norvegicus), UV-B lamp TLF72-100W/12 (Philips, 302 nm), RT-PCR machine (Bio-Rad CFX96), flow cytometer (BD FACSCalibur), centrifuge (Eppendorf 5804R), TFF filter (Repligen KrosFlo), Masson's Trichrome staining, and SPSS 26.0 for data analysis.

Main Findings: E-MSCs at 200 µL and 300 µL significantly increased p21 and Cyclin D gene expression in UV-B–induced collagen loss model in male Wistar rats. Highest expression was found in the 300 µL E-MSCs group. ANOVA and Kruskal–Wallis tests showed significant differences ($p < 0.05$) between treatment and control groups, confirming the therapeutic potential of E-MSCs in regulating gene expression related to skin regeneration.

Novelty/Originality of this study: This study is the first to investigate the in vivo effects of hypoxia-conditioned MSC-derived exosomes (E-MSCs) on both p21 and Cyclin D gene expression in a UV-B–induced collagen loss model. It advances existing knowledge by revealing the dual regulatory role of E-MSCs in cell cycle arrest and proliferation, contributing to innovative skin regeneration therapies.

Corresponding Author:
Riaflor Alcabedos,
Genetics and Molecular Biology Division, University of the Philippines Los Baños,
Brgy. Batong Malake, Los Baños, Laguna 4031 Philippines
Email: riafloralca@gmail.com

1. INTRODUCTION

Exposure to ultraviolet (UV) radiation, particularly UV-B (280–315 nm), is one of the most significant external factors contributing to premature skin aging and damage to the deeper layers of skin tissue. UV-B is known to induce oxidative stress through the generation of *Reactive Oxygen Species* (*ROS*), which play a major role in the degradation of key structural proteins such as collagen [1], [2]. Collagen, as a major component of the skin's extracellular matrix, plays a crucial role in maintaining skin integrity, mechanical strength, and elasticity [3], [4]. UV-B-induced collagen degradation leads to *collagen loss*, characterized by increased wrinkling, loss of skin elasticity, and the emergence of premalignant lesions or skin cancer [5], [6].

At the molecular level, elevated *ROS* levels due to UV-B exposure cause DNA damage, subsequently activating DNA damage sensor proteins such as *p53*. The activation of *p53* stimulates the expression of the *p21* (*CDKN1A*) gene, a cell cycle regulator that inhibits the activity of *Cyclin Dependent Kinases* (*CDKs*), particularly in the G1 phase [7]-[9]. This mechanism is a vital component of the cellular checkpoint system designed to prevent the proliferation of cells with damaged DNA [10], [11]. Concurrently, *cyclin D* also plays an important role in regulating the transition from the G1 to the S phase by forming a complex with *CDK4/6*, which facilitates the phosphorylation of the *retinoblastoma protein* (*pRb*), ultimately promoting the expression of proliferative genes such as *cyclin E*.

Chronic oxidative stress resulting from UV-B exposure not only induces cell cycle arrest through *p21* activation but also disrupts *cyclin D* expression, thereby indirectly slowing tissue regeneration and exacerbating *collagen loss* [12], [13]. The impaired function of fibroblasts in collagen synthesis further deteriorates the extracellular matrix, accelerating the skin aging process [14], [15]. In addition, inflammatory signaling pathways such as *NF-κB* and *SASP* (*senescence-associated secretory phenotype*) also mediate the expression of various inflammatory mediators such as *IL-6*, *IL-8*, and *MMPs*, which contribute to collagen degradation and inhibit tissue repair.

In recent years, exosome-based therapy derived from *Mesenchymal Stem Cells* (*MSCs*) has garnered significant attention in the fields of regenerative medicine and anti-aging. Exosomes are extracellular vesicles that carry various bioactive cargos including *miRNA*, *mRNA*, proteins, and lipids, which can modulate multiple molecular pathways in target cells [16], [17]. One of the advantages of MSC-derived exosomes is their ability to reduce *ROS*, inhibit inflammation, and enhance fibroblast proliferation and migration [18], [19]. Exosomes from MSCs cultured under hypoxic conditions (*E-MSCs hypoxia*) have demonstrated stronger therapeutic effects compared to those cultured under normoxic conditions [20], [21].

Previous studies have reported that exosomes isolated from umbilical cord blood stimulate wound closure by inducing collagen synthesis through the *TGF-β* signaling pathway at a dose of 20 µg [22]. This study differs from previous research in that *E-MSCs* will be treated on a collagen loss mouse model induced by UV-B radiation, and the expression of *p21* and *cyclin D* genes will be analyzed. Earlier studies also reported that exosomes lead to increased expression of *procollagen type I* and a significant decrease in *MMP-1* expression, primarily through the downregulation of *Tumor Necrosis Factor-Alpha* (*TNF-α*) and upregulation of *Transforming Growth Factor-Beta* (*TGF-β*) [23]. This study differs from previous research in that *E-MSCs* will be administered to a collagen loss mouse model induced by UV-B radiation, and the expression of *p21* and *cyclin D* genes will be analyzed. Earlier studies found that the administration of *MSC-derived exosomes* enhanced the production of *collagen A1* and prevented the degradation of the extracellular matrix [24].

Previous studies have reported that exosomes derived from *human adipose-derived MSCs* reduce extracellular matrix production through the downregulation of *TGF-β2* and *Notch-1* [25]. This study differs from previous research in that *E-MSCs* will be administered to a collagen loss mouse model induced by UV-B radiation, and the expression of *p21* and *cyclin D* genes will be analyzed. Previous studies have reported that exosomes derived from *human MSCs* inhibit collagen degradation by suppressing the expression of *collagen type I* and *III*, as well as by downregulating the expression of *α-SMA*, *MMP2*, *MMP13*, and *MMP14* [26]. This study differs from previous research in that *E-MSCs* will be administered to a collagen loss mouse model induced by UV-B radiation, and the expression of *p21* and *cyclin D* genes will be analyzed.

Based on this foundation, it can be assumed that subcutaneous administration of *E-MSCs hypoxia* in a UV-B-induced collagen loss mouse model has the potential to modulate the expression of *p21* and *cyclin D* genes. The modulation of these gene expressions serves as an important indicator in determining the effectiveness of exosome-based therapy for the repair and regeneration of skin tissue damaged by UV-B exposure. This research also provides scientific contributions to the development of non-immunogenic cellular therapy with high potential in the field of regenerative dermatology.

Therefore, this study aims to experimentally investigate the effects of *hypoxia-conditioned MSC-derived exosomes* on the expression of *p21* and *cyclin D* genes in a UV-B-induced collagen loss mouse model. By using an *in vivo* approach and gene expression analysis through *RT-qPCR*, the results of this study are expected to offer new insights into exosome-based regenerative therapies for skin conditions related to premature aging or damage due to ultraviolet radiation exposure.

2. RESEARCH METHOD

2.1 Type and Research Design

This study is an *in vivo* experimental research using a Post-Test Only Control Group Design and male *Rattus norvegicus* of the Wistar strain as experimental animals. This design allows for the evaluation of the effects of treatment with exosomes derived from *Mesenchymal Stem Cells* (*E-MSCs*) on the expression of *p21* and *Cyclin D* genes following UV-B radiation exposure. The study involved five treatment groups:

- K1: Normal control (*healthy rats without UV-B exposure*)
- K2: Negative control (*rats exposed to UV-B without treatment; administered 0.9% NaCl*)
- K3: Positive control (*rats exposed to UV-B; administered 200 µL Hyaluronic Acid*)
- K4: Treatment with *E-MSCs* 200 µL
- K5: Treatment with *E-MSCs* 300 µL

2.2 Subjects and Research Samples

The study used 30 male *Wistar* rats aged 2–3 months, weighing between 200–250 grams. The rats were randomly assigned (*randomized sampling*) into five treatment groups. The inclusion criteria included being in healthy condition and exhibiting *collagen loss* due to UV-B exposure. The exclusion criteria comprised anatomical abnormalities, a history of previous use in other studies, and absence of *collagen loss*. Rats that died or developed infections during the study were categorized as *dropouts*..

2.3 Experimental Treatments

The rats were exposed to narrowband UV-B radiation (*TLF72-100W/12, 302 nm*) at a dose of 160 mJ/cm² for 8 minutes per day on days 1, 2, 4, 5, and 7 over a period of two weeks. After validation of *collagen density* reduction, treatments were administered via subcutaneous injection for 14 consecutive days starting from day 15, according to the assigned groups.

Research Variables

- Independent variable: Dose of *E-MSCs* (200 µL and 300 µL)
- Dependent variables: Expression of *p21* and *Cyclin D* genes
- Preconditioning variable: Exposure to UV-B radiation
- Controlled variables: Rat strain, age, sex, body weight, and maintenance conditions

2.4 Research Procedure

The research procedure began with the isolation and characterization of *Mesenchymal Stem Cells* (*MSCs*) obtained aseptically from the umbilical cord. Characterization was carried out using surface markers *CD90*, *CD29*, *CD45*, and *CD31* through *flow cytometry* to ensure cell purity and identity. Once the cultured *MSCs* met the required criteria, exosomes (*E-MSCs*) were produced and isolated from the MSC cultures using *gradient centrifugation* and *tangential flow filtration* (*TFF*) methods.

Validation of *collagen loss* due to UV-B exposure was performed by staining skin tissues using the *Masson's Trichrome* method. Subsequently, *E-MSCs* were administered via subcutaneous injection to the treatment groups according to the predetermined doses. Skin tissue samples were collected on day 29 post-treatment to analyze the expression of *p21* and *Cyclin D* genes. The analysis was conducted using the *Reverse Transcriptase Polymerase Chain Reaction* (*RT-PCR*) method with specific primers and *SYBR Green* reagents, while gene expression was calculated relative to the *housekeeping gene GAPDH* as the reference [27], [28].

2.5 Data Analysis

Data were analyzed using SPSS version 26.0. Normality was tested using the *Shapiro–Wilk* test, and homogeneity was assessed using *Levene's test* [29], [30].

- If the data were normally distributed and homogeneous → *One-Way ANOVA* was performed, followed by *Tamhane's post hoc* test.
- If the data were not normally distributed → *Kruskal–Wallis* test was used, followed by the *Mann–Whitney* test.

  A p-value of < 0.05 was considered statistically significant.

3. RESULTS AND DISCUSSION

The research subjects were male *Wistar* rats weighing between 200–250 grams and aged 2–3 months, which were induced with UV-B radiation at 302 nm with an energy intensity of 160 mJ/cm². A total of 30 male rats were used, and no animals dropped out during the study. The experiment consisted of five groups: Group K1 served as the healthy control (rats without any treatment), Group K2 was the negative control (rats exposed to UV-B and given 0.9% *normal saline*), Group K3 was the positive control (rats exposed to UV-B and administered a subcutaneous injection of *Hyaluronic Acid* at a dose of 200 µL), Group K4 consisted of rats given subcutaneous injections of *E-MSCs* at a dose of 200 µL, and Group K5 received subcutaneous injections of *E-MSCs* at a dose of 300 µL.

Macroscopic observation was conducted to assess *collagen loss* resulting from UV-B exposure. The findings showed visible signs of *collagen loss* in rats exposed to UV-B radiation when compared to the unexposed control group, as illustrated in Figure 5.1. To further validate this observation, anatomical analysis was performed using *Masson's Trichrome* staining to examine the density of *elastin* fibers affected by UV-B

exposure. Based on previous research, *elastin* fibers can be identified as red structures when stained using *Masson's Trichrome*. The anatomical observation confirmed the presence of *collagen loss* following UV-B exposure, as shown in Figure 1.

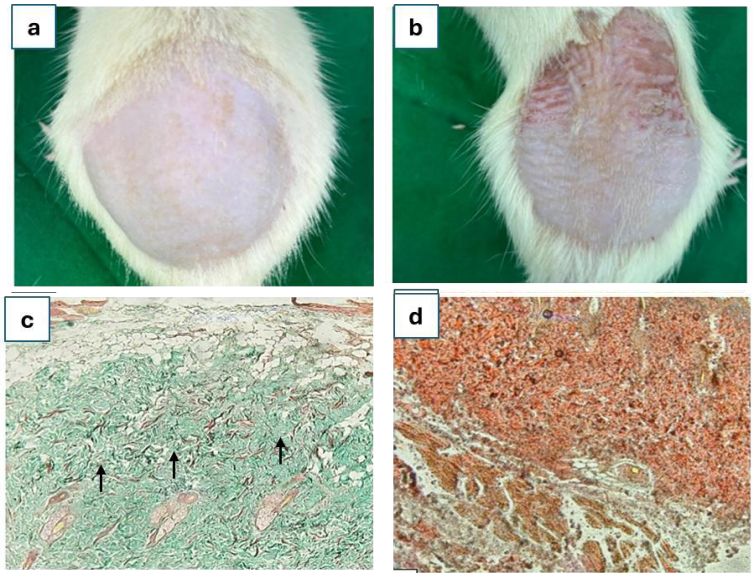

Figure 1. (A) Healthy control rat showing no erythema or wrinkling. (B) UV-B–exposed rat without treatment showing visible redness and skin wrinkling. (C) *Masson's Trichrome* staining with blue coloration indicating *collagen* production. (D) Skin of UV-B–exposed rat showing red coloration, indicating *collagen* degradation (*collagen loss*). *Black arrows indicate areas of collagen deposition.*

3.1. Validation Results of MSCs

The isolation of *Mesenchymal Stem Cells* (*MSCs*) was conducted at the Stem Cell and Cancer Research (SCCR) Laboratory, using umbilical cords from pregnant rats at gestational day 19. The isolated cells were cultured in specialized media within culture flasks. After the fourth passage, the cultured *MSCs* exhibited adherence to the bottom of the flask with a characteristic *spindle-shaped* morphology.

To confirm their multipotent differentiation potential, *MSCs* were cultured in osteogenic and adipogenic induction media for 14 days to assess their ability to differentiate into osteocytes and adipocytes. Microscopic observations at 100× and 200× magnification revealed that the cultured cells had an elongated, oval shape, a single round nucleus, prominent fibrous extensions resembling fibroblasts, and were *plastic-adherent* (Figure 2). Osteogenic differentiation of *MSCs* was indicated by the presence of calcium deposits stained with *Alizarin Red* (Figure 3a), while adipogenic differentiation was demonstrated by lipid droplet accumulation stained with *Oil Red O* (Figure 3b). The calcium and lipid deposits, representing successful differentiation into osteocytes and adipocytes respectively, were visualized as red-stained areas in each culture.

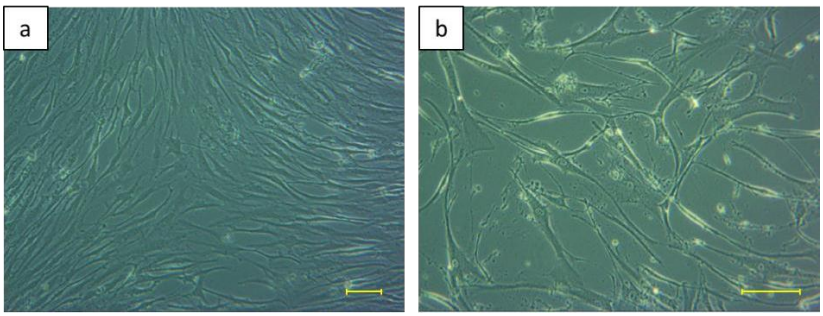

Figure 2. Morphological characteristics of isolated cells. The isolated cells exhibited typical *MSC*-like morphology, including oval to elongated shape, single round nucleus, and prominent fibrous extensions (*fibroblast-like*), observed under a light microscope at 100× magnification (a) and 200× magnification (b). Scale bar: 50 µm.

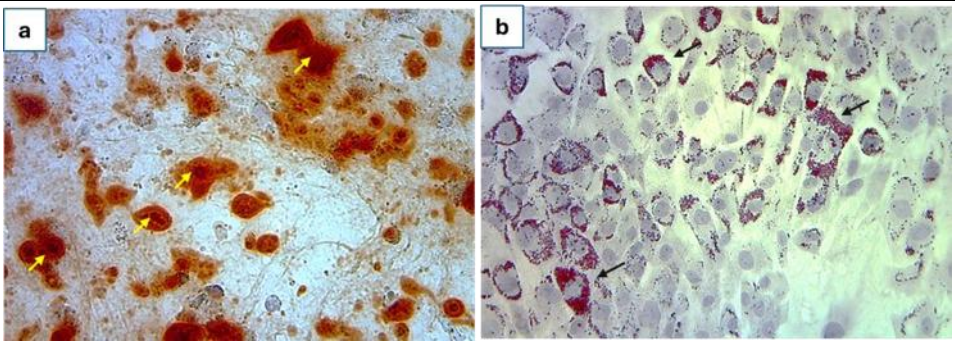

Figure 3. Differentiation potential of isolated cells. (a) The isolated cells demonstrated the ability to differentiate into osteocytes, as indicated by *Alizarin Red* staining, and (b) differentiated into adipocytes, as indicated by *Oil Red O* staining, observed at 400× magnification. *Yellow arrows indicate calcium deposits; black arrows indicate lipid droplets.*

The validation of *MSCs* isolation was performed using *flow cytometry* to demonstrate the cells' ability to express specific *surface markers*. Quantitative results showed high positive expression of *CD90.1* (99.8%) and *CD29* (97.7%), while negative expression was observed for *CD45* (1.9%) and *CD31* (3.7%) (Figure 4).

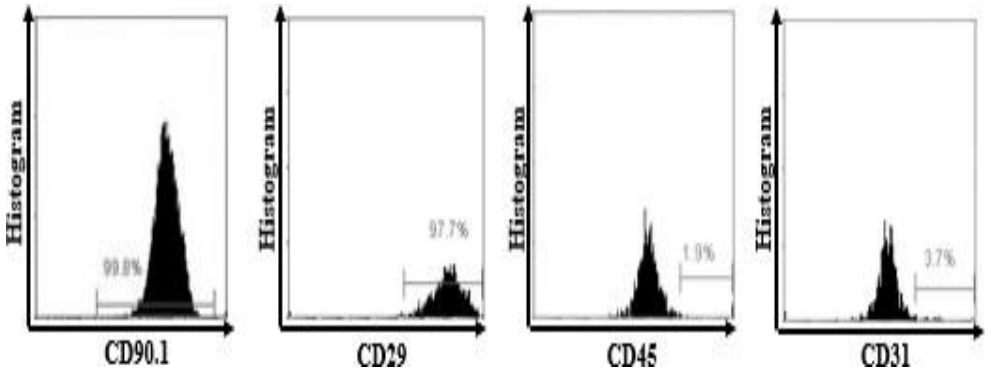

Figure 4. Flow cytometry analysis of isolated cells. The isolated cells exhibited high expression of *CD90.1* and *CD29*, and low expression of *CD45* and *CD31*

he *MSC* culture medium, presumed to contain *exosomes*, was filtered using the *Tangential Flow Filtration* (*TFF*) technique. The percentage of *exosomes* was then analyzed using the *flow cytometry* method. The analysis results indicated that the filtration technique successfully isolated *exosomes* at a proportion of 9.1% (Figure 5), with a mean *Mean Fluorescence Intensity* (*MFI*) value of 1056.35 and an average *exosome* concentration of 960 ng/mL.

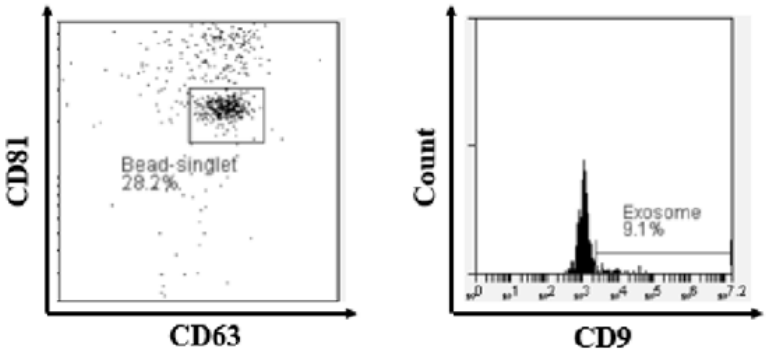

Figure 5. Flow cytometry analysis of *MSC*-derived exosomes. The *exosomes* formed a positive population for *CD81* and *CD63*, with 9.1% of the population also expressing *CD9*.

3.2. Effect of E-MSCs Administration on *p21* Gene Expression

The study on *Mesenchymal Stem Cell*-derived *exosomes* and their effects on *p21* and *Cyclin D* gene expression in male *Wistar* rats induced by UV-B exposure was conducted over a period of 28 days. The results of the study are presented in Table 1.

Table 1. Mean Values, Normality Test, and Homogeneity Test Results for *p21* and *Cyclin D* Gene Expression

Variable	Group					Sig. (p)
	K1 (n=6)	K2 (n=6)	K3 (n=6)	K4 (n=6)	K5 (n=6)	
p21 Expression						
Mean Std.deviasi	1.03 ± 0.01	0.28 ± 0.14	0.59 ± 0.23	0.73 ± 0.15	0.91 ± 0.32	
Shapiro Wilk*	0.167	0.733	0.151	0.433	0.275	
Levene test***						0.049
ANOVA*****					0.001*****	
Cyclin D Expression						
Mean Std.deviasi	1.04 ± 0.02	0.52 ± 0.25	0.74 ± 0.24	0.78 ± 0.19	0.84 ± 0.072	
Shapiro Wilk**	0.026	0.792	0.340	0.998	0.760	
Levene test****						0.007
Kruskall Wallis*****					0.004*****	

Note:
*Normal distribution p > 0.05
**Not normally distributed p < 0.05
***Homogeneous variance p > 0.05
****Not homogeneous variance p < 0.05
*****Significant difference p < 0.05

Table 1 shows that the lowest mean *p21* gene expression was found in the treatment group K2 (rats exposed to UV-B without treatment and administered 0.9% *NaCl*), followed by group K3 (rats exposed to UV-B and treated subcutaneously with 200 µL *Hyaluronic Acid*), then group K4 (rats exposed to UV-B and treated subcutaneously with 200 µL *E-MSCs*), and subsequently group K5 (rats exposed to UV-B and treated subcutaneously with 300 µL *E-MSCs*). The highest mean *p21* expression was observed in the healthy control group (K1).

The *Shapiro–Wilk* normality test showed that all groups had normally distributed *p21* expression data ($p > 0.05$). However, the *Levene's Test* for homogeneity indicated that the data were not homogeneous ($p < 0.05$). Therefore, the analysis was performed using *One-Way ANOVA*. The *One-Way ANOVA* test showed a statistically significant difference among the groups with a *p*-value of 0.001 ($p < 0.05$), followed by *Tamhane's post hoc* test to determine which specific groups had the most significant effects.

Table 2. Pairwise Comparison of *p21* Gene Expression Between Groups

Parameter	Group	Comparison Group	Sig.	95% Confidence Interval	
				Lower Bound	Upper Bound
p21 Expression	K1	K2	0.001	0.4875	1.0159
		K3*	0.050	-0.0002	0.8835
		K4*	0.037	0.0218	0.5882
		K5	0.995	-0.5016	0.7349
	K2	K3	0.190	-0.7214	0.1014
		K4*	0.003	-0.7389	-0.1544
		K5*	0.031	-1.2113	-0.5870
	K3	K4	0.944	-0.5505	0.2772
		K5	0.531	-0.9126	0.2626
	K4	K5	0.927	-0.7628	0.3862

*Post Hoc Tamhane test with significance value p<0.05

The results of the *Tamhane's post hoc* test presented in Table 2 show that *p21* gene expression in the healthy control group (K1) was significantly different from that in the UV-B–exposed untreated group (K2), with a *p*-value of 0.001 ($p < 0.05$). A significant difference was also observed between group K1 and the group treated subcutaneously with 200 µL *Hyaluronic Acid* (K3), with a *p*-value of 0.050 ($p < 0.05$), as well as between group K1 and the group treated subcutaneously with 200 µL *E-MSCs* (K4), with a *p*-value of 0.037 ($p < 0.05$).

Furthermore, a significant difference was observed between group K2 (UV-B–exposed without treatment) and group K4 (treated with 200 µL *E-MSCs*), with a *p*-value of 0.003 ($p < 0.05$), and between group K2 and group K5 (treated with 300 µL *E-MSCs*), with a *p*-value of 0.031 ($p < 0.05$).

Based on these results, it can be concluded that the administration of *E-MSCs* at doses of 200 µL and 300 µL significantly affects *p21* gene expression in UV-B–exposed male *Wistar* rats. Therefore, the research hypothesis is accepted.

3.2. Effect of E-MSCs Administration on *Cyclin D* Gene Expression

The lowest mean *Cyclin D* gene expression was observed in the treatment group K2 (rats exposed to UV-B without treatment, administered 0.9% *NaCl*), followed by group K3 (rats exposed to UV-B and treated subcutaneously with 200 µL *Hyaluronic Acid*), then group K4 (treated subcutaneously with 200 µL *E-MSCs*), and subsequently group K5 (treated subcutaneously with 300 µL *E-MSCs*). The highest mean *Cyclin D* expression was found in the healthy control group (K1).

Based on the *Shapiro–Wilk* test, *Cyclin D* expression data from all groups were not normally distributed ($p < 0.05$), and the *Levene's Test* indicated that the data were not homogeneous ($p < 0.05$). Therefore, data were analyzed using the *Kruskal–Wallis* test. The *Kruskal–Wallis* test revealed a statistically significant difference among the groups, with a *p*-value of 0.004 ($p < 0.05$), followed by the *Mann–Whitney* test to determine which specific groups showed the most significant effects.

Table 3. Pairwise Comparison of *Cyclin D* Gene Expression Between Groups

Parameter	Group	Comparison Group	Sig.
p21 Expression	K1	K2*	0.002
		K3*	0.041
		K4*	0.009
		K5*	0.02
	K2	K3	0.132
		K4	0.093
		K5*	0.041
	K3	K4	0.818
		K5	0.485
	K4	K5	0.485

The Mann–Whitney test was conducted to compare *Cyclin D* gene expression between groups, with a significance level set at $p < 0.05$.

The *Mann–Whitney* test results presented in Table 3 show that *Cyclin D* gene expression in the healthy control group (K1) differed significantly from the UV-B–exposed untreated group (K2), with a *p*-value of 0.002 ($p < 0.05$). A significant difference was also observed between group K1 and the group treated subcutaneously with 200 µL *Hyaluronic Acid* (K3), with a *p*-value of 0.041 ($p < 0.05$), between group K1 and the group treated with 200 µL *E-MSCs* (K4), with a *p*-value of 0.009 ($p < 0.05$), and between group K1 and the group treated with 300 µL *E-MSCs* (K5), with a *p*-value of 0.02 ($p < 0.05$). Additionally, a significant difference was found between group K2 (UV-B only) and group K5 (UV-B + 300 µL *E-MSCs*), with a *p*-value of 0.041 ($p < 0.05$).

Based on these findings, it can be concluded that administration of *E-MSCs* at both 200 µL and 300 µL significantly influenced *Cyclin D* gene expression in UV-B–exposed male *Wistar* rats, thereby supporting the acceptance of the research hypothesis. *Reactive Oxygen Species* (*ROS*) generated by UV-B exposure can cause DNA damage and induce the expression of *Matrix Metalloproteinases* (*MMPs*), which contribute to *collagen* degradation. This process is detected by DNA damage sensor proteins such as *ATM (Ataxia Telangiectasia Mutated)* and *ATR (ATM and Rad3-related)*. *ATM* and *ATR* are kinases that are activated in response to DNA damage and subsequently phosphorylate several target proteins, including *p53* [31].

Phosphorylation of *p53* by *ATM/ATR* enhances the stability and transcriptional activity of *p53*. Activated *p53* subsequently induces the expression of various target genes involved in the DNA damage response. In addition, *Reactive Oxygen Species* (*ROS*) can activate the enzyme *IκB kinase* (*IKK*). *IKK* then phosphorylates *IκB*, the inhibitor of *NF-κB*. Phosphorylation of *IκB* leads to its proteasomal degradation, thereby releasing *NF-κB*, which can induce the expression of *Matrix Metalloproteinases* (*MMPs*) that promote *collagen* degradation. *NF-κB* subsequently translocates into the nucleus and induces the transcription of target genes such as *SMAD2/3* and activates *SMAD4*.

Phosphorylated *SMAD2/3* forms a heteromeric complex with *SMAD4*, which translocates into the nucleus. Within the nucleus, this complex functions as a transcription factor regulating the expression of target genes. One of the primary genes induced by the *SMAD2/3/4* complex is *p21 (CDKN1A)*, a cell cycle inhibitor that suppresses *cyclin-dependent kinase* (*CDK*) activity, thereby controlling cell cycle progression. *p21* induces cell cycle arrest at the G1/S phase, preventing cell proliferation. The reduction in *collagen* production by fibroblasts as a result of *p21*-induced cell cycle arrest may contribute to extracellular matrix degradation or thinning.

On the other hand, *Reactive Oxygen Species* (*ROS*) generated by UV-B can activate the *Mitogen-Activated Protein Kinase* (*MAPK*) pathway. The three main *MAPK* pathways involved are *ERK* (extracellular signal-regulated kinase), *JNK* (*c-Jun N-terminal kinase*), and *p38 MAPK*. Activation of *JNK*, in particular, leads to the phosphorylation and activation of *c-Jun*, a component of the *Activator Protein-1 (AP-1)* transcription factor. *AP-1* can induce the expression of *Matrix Metalloproteinases (MMPs)*, which trigger *collagen* degradation. The *AP-1* complex, composed of *c-Jun* and *c-Fos*, binds to *AP-1 response elements* in the promoter regions of target genes, including *Cyclin D*. Activation of *AP-1* by the *c-Jun/c-Fos* complex enhances the transcription of *Cyclin D*, which in turn promotes cell cycle progression and fibroblast proliferation.

Analysis results demonstrated that the administration of *E-MSCs* at a dose of 300 µL significantly increased *p21* gene expression. This effect is presumed to be due to the bioactive compounds secreted by *E-MSCs*, which are typically classified as cytokines, chemokines, cell adhesion molecules, lipid mediators, interleukins (ILs), growth factors (GFs), hormones, exosomes, microvesicles, anti-inflammatory factors, and others [32], [33]. These factors are considered key mediators that participate in tissue repair and regeneration through paracrine mechanisms that mediate cell-to-cell signaling. In the context of skin regeneration, one of the critical cytokines involved is *Transforming Growth Factor Beta* (*TGF-β*) [34]. *TGF-β* plays a key role as a regulator of *procollagen I* synthesis [35].

Furthermore, *TGF-β* induces a delayed activation of the *ERK signaling pathway* [35], [36]. On the other hand, *TGF-β* inhibits *Protein Kinase A* (*PKA*), thereby preventing the activation of *CREB* (*cAMP response element-binding protein*) and the subsequent activation of *Matrix Metalloproteinases* (*MMPs*), resulting in the inhibition of collagen degradation.[37]. The high *IL-10* content in *exosomes* can inhibit *ROS* production, thereby reducing inflammation and suppressing *p53* activation [38], [39]. When DNA damage occurs, *p53* signals the gene encoding the *p21* protein, leading to its production. *p21* inhibits cell cycle progression, thereby preventing the replication of damaged cells. Cell cycle arrest also provides time for DNA repair. Once the damage is repaired, the cell cycle resumes and proceeds with the duplication of healthy cells.

Analysis results also demonstrated that administration of *E-MSCs* at a dose of 300 µL significantly increased *Cyclin D* gene expression. This is likely due to the presence of various bioactive molecules within *E-MSCs*, including proteins, RNA (mRNA, miRNA), lipids, and other signaling factors. *Exosomes* derived from MSCs can reduce *ROS* production and oxidative damage in various cell types, including keratinocytes and skin cells exposed to UV-B radiation. The *miRNA* content within exosomes may enhance the expression of the *CCND1* gene or *Cyclin D* protein either by promoting transcriptional activity or by inhibiting *Cyclin D* repressors.

This study presents a novel approach by utilizing umbilical cord-derived *exosome-mesenchymal stem cells* (E-MSCs) to repair UV-B–induced skin damage through molecular regulation of p21 and Cyclin D gene expression. The subcutaneous administration of E-MSCs significantly increased the expression of p21, a cell cycle inhibitor involved in DNA damage response, and Cyclin D, a key regulator of fibroblast proliferation and cell cycle progression. This suggests that E-MSCs possess a dual role in promoting skin regeneration and preventing further tissue degradation. The use of SYBR Green–based RT-qPCR with GAPDH as a reference gene to quantify the therapeutic effects of E-MSCs on these molecular markers is a rare application in skin regeneration studies. Furthermore, the study builds upon previous findings that exosomes derived from MSCs contain bioactive molecules such as microRNAs, cytokines (e.g., TGF-β and IL-10), and growth factors, which can modulate oxidative stress and inflammatory responses [40], [41].

In terms of implications, this research provides significant contributions to the development of anti-aging and regenerative therapies based on exosome biology, particularly for treating oxidative damage caused by UV-B radiation. The findings support the potential of E-MSCs as a cell-free therapeutic alternative with fewer immunological risks and broader clinical applicability. Moreover, this research has pedagogical value in the field of biology education, where it can be integrated into molecular biology, histology, and biotechnology curricula as a real-world example of gene expression regulation, stem cell therapy, and modern genetic analysis techniques such as RT-qPCR and flow cytometry. Thus, the study contributes not only to the advancement of biomedical science but also to the promotion of inquiry-based, research-oriented biological education.

A limitation of this study is the lack of analysis of key signaling pathways through which *E-MSCs* may inhibit *Reactive Oxygen Species* (*ROS*), such as the *SIRT1/PGC1α*, *PI3K/Akt/MAPK*, or *NF-κB* pathways. The biochemical pathways involved in antioxidant responses and *collagen* degradation are highly complex. This study may not fully capture the interactions between these pathways or other contributing factors. Further research is required to elucidate the detailed molecular mechanisms involved.

4. CONCLUSION

This study demonstrated a significant increase in *p21* gene expression in a UV-B–induced collagen loss rat model following subcutaneous administration of *E-MSCs* at a dose of 300 µL, compared to the in vivo control group. In addition, *Cyclin D* gene expression also showed a significant increase in the same model after

E-MSCs treatment when compared to the control group. Future research is encouraged to further investigate the key signaling pathways involved in the mechanism of *E-MSCs*, particularly in their ability to inhibit *Reactive Oxygen Species* (*ROS*). Such investigations are essential to determine whether the underlying mechanism involves the *SIRT1/PGC1α*, *PI3K/Akt/MAPK*, or *NF-κB* pathways.

ACKNOWLEDGEMENTS

The authors would like to express their deepest gratitude to all individuals who contributed to the completion of this research. Special thanks are extended to those who provided technical assistance, guidance, and support during the laboratory procedures, data collection, and analysis. The authors also appreciate the constructive feedback and encouragement from peers and colleagues throughout the course of the study. Their insights and suggestions greatly enhanced the quality of this research.

REFERENCES

[1] M. Wei, X. He, N. Liu, and H. Deng, "Role of reactive oxygen species in ultraviolet-induced photodamage of the skin," *Cell Div.*, vol. 19, no. 1, pp. 1–9, 2024, doi: 10.1186/s13008-024-00107-z.

[2] A. Sajeeda *et al.*, "Seabuckthorn pulp extract alleviates UV-B-induced skin photo-damage by significantly reducing oxidative stress-mediated endoplasmic reticulum stress and DNA Damage in human primary skin fibroblasts and Balb/c mice skin," *Environ. Sci. Pollut. Res.*, vol. 31, no. 34, pp. 46979–46993, 2024, doi: 10.1007/s11356-024-34219-4.

[3] H. Park *et al.*, "Extracellular matrix-bioinspired anisotropic topographical cues of electrospun nanofibers: a strategy of wound healing through macrophage polarization," *Adv. Healthc. Mater.*, vol. 13, no. 12, May 2024, doi: 10.1002/adhm.202304114.

[4] A. Berdiaki, M. Neagu, P. Tzanakakis, I. Spyridaki, S. Pérez, and D. Nikitovic, "Extracellular matrix components and mechanosensing pathways in health and disease," *Biomolecules*, vol. 14, no. 9, p. 1186, Sep. 2024, doi: 10.3390/biom14091186.

[5] E. Csekes and L. Račková, "Skin aging, cellular senescence and natural polyphenols," *Int. J. Mol. Sci.*, vol. 22, no. 23, p. 12641, Nov. 2021, doi: 10.3390/ijms222312641.

[6] J. Flieger, M. Raszewska-Famielec, E. Radzikowska-Büchner, and W. Flieger, "Skin protection by carotenoid pigments," *Int. J. Mol. Sci.*, vol. 25, no. 3, p. 1431, Jan. 2024, doi: 10.3390/ijms25031431.

[7] E. Manousakis, C. M. Miralles, M. G. Esquerda, and R. H. G. Wright, "CDKN1A/p21 in breast cancer: part of the problem, or part of the solution?," *Int. J. Mol. Sci.*, vol. 24, no. 24, p. 17488, Dec. 2023, doi: 10.3390/ijms242417488.

[8] K. Engeland, "Cell cycle regulation: p53-p21-RB signaling," *Cell Death Differ.*, vol. 29, no. 5, pp. 946–960, 2022, doi: 10.1038/s41418-022-00988-z.

[9] M. Fischer, A. E. Schade, T. B. Branigan, G. A. Müller, and J. A. DeCaprio, "Coordinating gene expression during the cell cycle," *Trends Biochem. Sci.*, vol. 47, no. 12, pp. 1009–1022, 2022, doi: 10.1016/j.tibs.2022.06.007.

[10] L. Zhu, J. Liu, J. Chen, and Q. Zhou, "The developing landscape of combinatorial therapies of immune checkpoint blockade with DNA damage repair inhibitors for the treatment of breast and ovarian cancers," *J. Hematol. Oncol.*, vol. 14, no. 1, pp. 1–19, 2021, doi: 10.1186/s13045-021-01218-8.

[11] C. Q. X. Yam, H. H. Lim, and U. Surana, "DNA damage checkpoint execution and the rules of its disengagement," *Front. Cell Dev. Biol.*, vol. 10, no. October, pp. 1–15, 2022, doi: 10.3389/fcell.2022.1020643.

[12] Z. Zhang, R. Tan, Z. Xiong, Y. Feng, and L. Chen, "Dysregulation of autophagy during photoaging reduce oxidative stress and inflammatory damage caused by UV," *Front. Pharmacol.*, vol. 16, no. May, pp. 1–27, 2025, doi: 10.3389/fphar.2025.1562845.

[13] M. Zhang *et al.*, "Exploring mechanisms of skin aging: insights for clinical treatment," *Front. Immunol.*, vol. 15, no. November, pp. 1–23, 2024, doi: 10.3389/fimmu.2024.1421858.

[14] G. J. Fisher *et al.*, "Skin aging from the perspective of dermal fibroblasts: the interplay between the adaptation to the extracellular matrix microenvironment and cell autonomous processes," *J. Cell Commun. Signal.*, vol. 17, no. 3, pp. 523–529, Sep. 2023, doi: 10.1007/s12079-023-00743-0.

[15] N. N. Potekaev *et al.*, "The role of extracellular matrix in skin wound healing," *J. Clin. Med.*, vol. 10, no. 24, p. 5947, Dec. 2021, doi: 10.3390/jcm10245947.

[16] M. Y. Waqas *et al.*, "Extracellular vesicles and exosome: insight from physiological regulatory perspectives," *J. Physiol. Biochem.*, vol. 78, no. 3, pp. 573–580, 2022, doi: 10.1007/s13105-022-00877-6.

[17] M. A. Kumar *et al.*, "Extracellular vesicles as tools and targets in therapy for diseases," *Signal Transduct. Target. Ther.*, vol. 9, no. 1, 2024, doi: 10.1038/s41392-024-01735-1.

[18] D. Bian, Y. Wu, G. Song, R. Azizi, and A. Zamani, "The application of mesenchymal stromal cells (MSCs) and their derivative exosome in skin wound healing: a comprehensive review," *Stem Cell Res. Ther.*, vol. 13, no. 1, pp. 1–17, 2022, doi: 10.1186/s13287-021-02697-9.

[19] C. Zhou *et al.*, "Stem cell-derived exosomes: emerging therapeutic opportunities for wound healing," *Stem Cell Res. Ther.*, vol. 14, no. 1, pp. 1–18, 2023, doi: 10.1186/s13287-023-03345-0.

[20] S. Rautiainen, T. Laaksonen, and R. Koivuniemi, "Angiogenic effects and crosstalk of adipose-derived mesenchymal stem/stromal cells and their extracellular vesicles with endothelial cells," *Int. J. Mol. Sci.*, vol. 22, no. 19, p. 10890, Oct. 2021, doi: 10.3390/ijms221910890.

[21] Z. Ji *et al.*, "Oct4-dependent FoxC1 activation improves the survival and neovascularization of mesenchymal stem cells under myocardial ischemia," *Stem Cell Res. Ther.*, vol. 12, no. 1, pp. 1–23, 2021, doi: 10.1186/s13287-021-02553-w.

[22] Y. Zhang *et al.*, "Exosomes derived from human umbilical cord blood mesenchymal stem cells stimulate regenerative

wound healing via transforming growth factor-β receptor inhibition," *Stem Cell Res. Ther.*, vol. 12, no. 1, pp. 1–14, 2021, doi: 10.1186/s13287-021-02517-0.

[23] S. Hu *et al.*, "Needle-free injection of exosomes derived from human dermal fibroblast spheroids ameliorates skin photoaging.," *Physiol. Behav.*, vol. 176, no. 3, pp. 139–148, 2019, doi: 10.1021/acsnano.9b04384.Extra.

[24] Y. You *et al.*, "Intradermally delivered mRNA-encapsulating extracellular vesicles for collagen-replacement therapy," *Nat. Biomed. Eng.*, vol. 7, no. 7, pp. 887–900, 2023, doi: 10.1038/s41551-022-00989-w.

[25] J. Li, Z. Li, S. Wang, J. Bi, and R. Huo, "Exosomes from human adipose-derived mesenchymal stem cells inhibit production of extracellular matrix in keloid fibroblasts via downregulating transforming growth factor-β2 and Notch-1 expression," *Bioengineered*, vol. 13, no. 4, pp. 8515–8525, 2022, doi: 10.1080/21655979.2022.2051838.

[26] R. Tutuianu, A.-M. Rosca, D. M. Iacomi, M. Simionescu, and I. Titorencu, "Human mesenchymal stromal cell-derived exosomes promote in vitro wound healing by modulating the biological properties of skin keratinocytes and fibroblasts and stimulating angiogenesis," *Int. J. Mol. Sci.*, vol. 22, no. 12, p. 6239, Jun. 2021, doi: 10.3390/ijms22126239.

[27] N. Kwon, K. E. Lee, M. Singh, and S. G. Kang, "Suitable primers for GAPDH reference gene amplification in quantitative RT-PCR analysis of human gene expression," *Gene Reports*, vol. 24, p. 101272, 2021, doi: https://doi.org/10.1016/j.genrep.2021.101272.

[28] A. Caballero-Solares, J. R. Hall, X. Xue, and M. L. Rise, "Reverse Transcription-Quantitative Real-Time Polymerase Chain Reaction (RT-qPCR) for Gene Expression Analyses BT - Cancer Cell Biology: Methods and Protocols," S. L. Christian, Ed., New York, NY: Springer US, 2022, pp. 319–340. doi: 10.1007/978-1-0716-2376-3_21.

[29] M. Fiandini, A. B. D. Nandiyanto, D. F. Al Husaeni, D. N. Al Husaeni, and M. Mushiban, "How to calculate statistics for significant difference test using SPSS: understanding students comprehension on the concept of steam engines as power plant," *Indones. J. Sci. Technol.*, vol. 9, no. 1, pp. 45–108, 2024, doi: 10.17509/ijost.v9i1.64035.

[30] B. K. Blajvaz, I. Z. Bogdanović, T. S. Jovanović, J. D. Stanisavljević, and M. V. Pavkov-Hrvojević, "The jigsaw technique in lower secondary physics education: students' achievement, metacognition and motivation," *J. Balt. Sci. Educ.*, vol. 21, no. 4, pp. 545–557, 2022, doi: 10.33225/jbse/22.21.545.

[31] P. T. Pugliese, *Physiology of the Skin II: An Expanded Scientific Guide for the Skin Care Professional*. Allured Publishing Corporation, 2001. [Online]. Available: https://books.google.co.id/books?id=WOSYPQAACAAJ

[32] C. Harrell, C. Fellabaum, N. Jovicic, V. Djonov, N. Arsenijevic, and V. Volarevic, "Molecular mechanisms responsible for therapeutic potential of mesenchymal stem cell-derived secretome," *Cells*, vol. 8, no. 5, p. 467, May 2019, doi: 10.3390/cells8050467.

[33] D. Kyurkchiev, "Secretion of immunoregulatory cytokines by mesenchymal stem cells," *World J. Stem Cells*, vol. 6, no. 5, p. 552, 2014, doi: 10.4252/wjsc.v6.i5.552.

[34] L. Wang *et al.*, "Transforming growth factor β plays an important role in enhancing wound healing by topical application of Povidone-iodine," *Sci. Rep.*, vol. 7, no. 1, pp. 1–8, 2017, doi: 10.1038/s41598-017-01116-5.

[35] P.-S. Lin *et al.*, "Transforming growth factor beta 1 increases collagen content, and stimulates procollagen I and tissue inhibitor of metalloproteinase-1 production of dental pulp cells: Role of MEK/ERK and activin receptor-like kinase-5/Smad signaling," *J. Formos. Med. Assoc.*, vol. 116, no. 5, pp. 351–358, May 2017, doi: 10.1016/j.jfma.2016.07.014.

[36] D.-S. Kim, S.-H. Park, and K.-C. Park, "Transforming growth factor-β1 decreases melanin synthesis via delayed extracellular signal-regulated kinase activation," *Int. J. Biochem. Cell Biol.*, vol. 36, no. 8, pp. 1482–1491, Aug. 2004, doi: 10.1016/j.biocel.2003.10.023.

[37] H. Yang, G. Li, J.-J. Wu, L. Wang, M. Uhler, and D. M. Simeone, "Protein kinase a modulates transforming growth factor-β signaling through a direct interaction with Smad4 protein," *J. Biol. Chem.*, vol. 288, no. 12, pp. 8737–8749, Mar. 2013, doi: 10.1074/jbc.M113.455675.

[38] P. S. Siebenga, G. van Amerongen, E. S. Klaassen, M. L. de Kam, R. Rissmann, and G. J. Groeneveld, "The ultraviolet B inflammation model: Postinflammatory hyperpigmentation and validation of a reduced UVB exposure paradigm for inducing hyperalgesia in healthy subjects," *Eur. J. Pain (United Kingdom)*, vol. 23, no. 5, pp. 874–883, 2019, doi: 10.1002/ejp.1353.

[39] Y. Gao, D. Tu, R. Yang, C. H. Chu, H. M. Gao, and J. S. Hong, "Through reducing ROS production, IL-10 suppresses caspase-1-dependent IL-1β maturation, thereby preventing chronic neuroinflammation and neurodegeneration," *Int. J. Mol. Sci.*, vol. 21, no. 2, pp. 1–15, 2020, doi: 10.3390/ijms21020465.

[40] D. G. Phinney and M. F. Pittenger, "Concise review: MSC-derived exosomes for cell-free therapy," *Stem Cells*, vol. 35, no. 4, pp. 851–858, Apr. 2017, doi: 10.1002/stem.2575.

[41] J. Li, J. Wang, and Z. Chen, "Emerging role of exosomes in cancer therapy: progress and challenges.," *Mol. Cancer*, vol. 24, no. 1, p. 13, Jan. 2025, doi: 10.1186/s12943-024-02215-4.